

<https://doi.org/10.37501/soilsa/176686>

# Distribution of iron forms in different types of black earths in the Chełmno Lake District, northern Poland, as an indicator of soil-forming process

Mateusz Pawłowski\*, Mirosław Kobierski

Bydgoszcz University of Science and Technology, Faculty of Agriculture and Biotechnology, Department of Biogeochemistry and Soil Science, Bernardyńska St. 6, 85-029 Bydgoszcz, Poland

\* mgr inż. Mateusz Pawłowski, matpaw007@pbs.edu.pl, ORCID ID: <https://orcid.org/0000-0003-0293-5806>

## Abstract

Received: 2023-04-16  
Accepted: 2023-12-09  
Published online: 2023-12-09  
Associated editor: J. Waroszewski

## Keywords:

Black earths  
Iron  
Soil-forming processes  
Phaeozems  
Gleyic process

An important part of soil science research is the classification of soils. Numerous soil scientists have paid special attention to various dependencies related to the content and distribution of iron forms in the soil profile. This allows the taxonomic unit to be determined according to soil classifications. The research objective was to evaluate the distribution of iron forms as an indicator of soil-forming processes in four profiles of arable black earths. The research subject was soils formed from glacial sediments in the Chełmno Lake District (northern Poland). They were determined by morphological description to be Phaeozems representing four subtypes: Haplic Phaeozem, Luvic Gleyic Phaeozem, Gleyic Phaeozem and Gleyic (Cambic) Phaeozem. Soil horizons were described according to FAO guidelines. The soil samples were analysed for the content of free iron oxides ( $Fe_o$ ) according to Mehra and Jackson's method, as well as the content of amorphous iron oxides, ( $Fe_a$ ) according to Schwertmann's method. Based on the content of  $Fe_a$  and  $Fe_o$ , the content of crystalline iron oxides ( $Fe_c$ ) was calculated using the formula:  $Fe_c = Fe_a - Fe_o$  and the iron oxides activity index was calculated from the  $Fe_o/Fe_a$  ratio. The content of  $Fe_c$  was highest in the Bt horizon of profile II. In individual profiles,  $Fe_a$  content was highest in the Bt horizon of gleyic Phaeozem and the AB horizon of gleyic (cambic) Phaeozem. In Luvic Gleyic Phaeozem and Gleyic (Cambic) Phaeozem iron was removed from the surface horizon to be accumulated in the illuvial horizon. The uniformity of content of total iron and its free iron oxides in the parent material of the analysed soils indicates its genetic homogeneity. The release of iron in the Ap horizon is characteristic of chemical weathering. The relationship between the content of  $Fe_o$  and  $Fe_a$  determines the degree of crystallization of free iron oxides. Based on the statistical analysis, a significantly positive correlation between the content of clay fraction and all the iron forms determined was found. All the profiles were characterized by similar degrees of weathering of the soil material, which was determined on the basis of the  $Fe_a/Fe_c$  ratio. The soils also demonstrate a low value of iron mobilization, as confirmed by the values of the  $Fe_a/Fe_c$  ratio. Determining iron forms and interpreting analysis results help in the correct classification of soils, because the distribution of iron forms in soil profiles depends mainly on pedogenesis.

## 1. Introduction

Detailed description of soil properties is essential because it serves as a basis for soil identification and classification. Field morphology of a soil profile and precise descriptions of features for each horizon are often not confirmed by the results of laboratory analysis. The soil formation process are mainly determined by the properties of the parent material, climatic conditions and vegetation (Targulian and Krasilnikov, 2007). The origin of the parent material is a contributing factor to the spatial variability of soil cover; this variability is a natural property that derives from the diversity of soil factors and the overlapping of soil-

forming processes (Bockheim et al, 2005; Łabaz et al, 2018). Parent materials are the passive soil-forming factors responsible for the formation of soil through their mineralogical composition, texture, and stratification. The soil-forming factors of parent material and topography are largely site-related. Relatively fine-textured parent materials in temperate climate yield soil B horizons that tend to become redder and more clay-rich over time. Konecka-Betley et al. (2002) determined that the most important determinant of typological differentiation of soils is relief.

Iron plays an important role in the classification of soils because the vertical distribution of its forms in the soil profile depends mainly on pedogenesis (Chojnicki, 2010; Róžański et

al., 2013; Orzechowski et al., 2018). Iron released to the environment undergoes further alterations. The total iron ( $Fe_t$ ) content in soil consists of silicate and non-silicate forms, and free iron ( $Fe_o$ ) is mainly composed of more or less hydrated mineral forms of iron oxides, which occur in crystalline ( $Fe_c$ ) or amorphous ( $Fe_a$ ) forms. Complex compounds with which iron forms unstable bonds with humic substances are also considered to be free iron. The degree of weathering and formation of pedogenic iron oxides and hydroxides is expressed by the  $Fe_a/Fe_c$  ratio. An increasing value of  $Fe_a/Fe_c$  ratio reflects the progressive weathering of Fe (Arduino et al., 1986; Bednarek and Pokojska, 1996; Jankowski et al., 2011; Jankowski, 2014a, 2014b).  $Fe_a/Fe_c$  ratios described the transformation of iron in primary minerals into pedogenic iron oxides. This ratio usually increases with time. Transformations of iron can be inferred from the ratio of oxalate to dithionite-extractable iron ( $Fe_o/Fe_d$ ), which defines the relationship between the content of the most active forms of iron and its non-silicate forms (Schwertmann, 1988). That ratio indicates the degree of iron oxide crystallinity and can be used as a reliable indicator of soil-forming processes (McFadden and Hendricks, 1985). Values of the  $Fe_o/Fe_d$  ratio range from about 0 to 1. The high activity of iron oxides and the low degree of their crystallization may result from the high content of organic matter and alkaline pH (Schwertmann et al., 1986).  $Fe_o$  in the form of poorly crystalline Fe oxyhydroxides (e.g., ferrihydrite) is most often associated with clay minerals and occurs in the form of durable bonds with humus (Cornell and Schwertmann, 1996). Iron is chemically and microbiologically transformed, especially in soils rich in organic matter (Gliński and Stepniewska, 1986). Iron-reducing and iron-oxidizing microorganisms obtain energy through iron reduction or oxidation and thus play an important role in the metal's biogeochemical cycle (Roden et al., 2004). Free iron oxides exist in diffuse form or, if they form complex connections with the clay fraction, are responsible for the specific colour of the soil (Haidouti and Massas, 1998). Soil colour (hue, value, chroma) is known to reflect the type and proportion of iron oxides present, and many scientists use the colour of horizons to verify and interpret soil-forming processes (Bigham et al., 1991; Scheinost and Schwertmann, 1999; Aitkenhead et al., 2013; Vodyanitskii et al., 2018). The appearance of Fe mottles and Fe concretions in wet conditions indicates the occurrence of an iron hydroxides formation process. The Munsell colour chart is used for soil-horizon diagnostics in soil classification (IUSS Working Group WRB, 2022). Soil colour is a unique identification parameter that provides information about iron content, since this metal is one a major chromophore. This allows the distribution of iron through a soil profile (pedotransfer functions) to be assessed.

Numerous soil scientists have paid special attention to various dependencies related to the content and distribution of iron forms in the soil profile (Dąbkowska-Naskręt et al., 1997; Degórski, 2011; Jelić et al., 2011; Hu et al., 2013; Jaworska et al., 2016; Orzechowski et al., 2018), and this allows the taxonomic unit to be determined according to national or international soil classifications. In Central Europe some of the soils are derived from glacial till and reflect fine-textured, alkaline soil conditions in parent material and occur in variable forms, respectively to

position in the landscape, climate conditions, and land use. Disturbances, such as the impact of drainage systems and periods of drought caused by global warming cause groundwater levels to drop, which in turn increases the mineralization of organic matter and carbon dioxide emissions into the atmosphere. Although black earths (equivalent of Gleyic Phaeozems according to WRB (IUSS Working Group WRB, 2022)) cover only ~2.0% of the arable land in Poland, they store relatively high amounts of organic carbon in the soil.

Geomorphological processes and parent material are the main factors controlling the spatial mosaic of Phaeozems in Poland (Łabaz and Kabała, 2014). The variability of Phaeozems is also dependent upon the pedogenesis and age of soil (Eckmeier et al., 2007; Łabaz et al., 2018; Kabała, 2019; Kabała et al., 2019b; Łabaz et al., 2019). These soils at various stages of their transformation are placed in Phaeozems, Chernozems, or Kastanozems in classification acc. World Reference Base for Soil Resources (IUSS working group WRB, 2022). Chernozems can evolve towards in to Phaeozems. Both reference soil groups have a Mollic horizon with a base saturation of at least 50% as a diagnostic horizon. Compared to Chernozems, Luvisols occur in more humid regions, are more leached and therefore lacking carbonates in topsoil. With increasing precipitation and leaching, the translocation of clay covered with humic material started and may lead to transformation of Chernozems into Phaeozems or Luvisols. The argic B horizons seem to be relics fromof stronger leaching and indicate the development towards Luvisols (Eckmeier et al., 2007). Phaeozems are characterized by a humus-rich surface layer, and they are highly arable soils. Soil-forming process occurring in Gleyic Phaeozems may lead to transformation of these soils into Haplic/Luvisols Phaeozems or with cambic diagnostic horizon. Phaeozems are represented by several subtypes with varying thickness of the humic horizon, degree of leaching and water table depth. They are often slightly leached with neutral to moderately acidic pH in the surface horizon and alkaline pH in the parent material (Habel et al., 2007; Łabaz and Kabała, 2014; Kaczmarek et al., 2015; Kobierski et al., 2015; Hristov, 2020). Morphological features identified during field descriptions pose problems in the accurate classification of Phaeozems because they lack the Fe-based redoximorphic features (Thompson et al., 2006). They make it possible to determine the general depth and duration of anoxic conditions resulting from periodic soil saturation and reduction. A periodically waterlogged soil shows the characteristic redoximorphic features of Fe cycling between oxidized and reduced soil environments. The high Fe contents in most soils lead to high concentrations of iron oxides in soil solutions under reducing conditions. Iron is a relatively abundant constituent of soil, and the effects of iron transformation are usually reflected in soil morphology. The redox-dynamic soil environments typically have high rates of biological activity. Roden et al. (2004) suggest that oxidative saturation of organic-rich soil solutions promotes the formation of aqueous organic-Fe complexes and amorphous solids. The methods for describing the soil-forming processes also include analyses of sedimentological and granulometric indices and clay mineral composition (Zagórski, 1996; Długosz et al., 2009; Kobierski and Długosz, 2011; Drewnik, 2014; Jaworska et al., 2014, Kabała et al., 2022).

The aim of the study was to determine the effect of litho- and pedogenesis on the formation of black earths from Vistula glaciation sediments on the base of the profile distribution of iron in relation to texture and the physical and chemical properties of soils.

2. Materials and methods

The research subject were soils formed from glacial sediments (Poznań phase of Weichselian glaciation) within the Chełmno Lake District (Fig. 1), near Papowo Biskupie village (northern Poland). The studied soils were located in drained arable lands. The geographic location and information on the relief are shown in Table 1. According to their morphological features investigated soils were classified to Phaeozems (Fig. 2) representing four subtypes various forms of development: profile I – Haplic Phaeozem, profile II – Luvic Gleyic Phaeozem, profile III – Gleyic Phaeozem, profile IV – Gleyic (Cambic) Phaeozem (IUSS Working Group WRB 2022). Soil horizons were described according to FAO guidelines, suited to Central European conditions (Świtoniak et al., 2018). According to Polish Soil Classification (2019) they were determined as: profile I – leached black earths, profile II – clay-illuvial black earths, profile III – typical black earths, profile IV – cambic black earths.

Samples of soils with disturbed structure were taken from each of the designated genetic levels. Samples with undisturbed structure were also taken to determine bulk density. The following parameters were determined in the soil samples:

- the texture class using the Casagrande areometric method (ISO 11277: 2005), with results interpreted according to PTG (2009) and USDA classification, adopted by WRB (IUSS Working Group WRB 2022),
- the total content of organic carbon (TOC) using a Vario Max analyser by Elementar (Germany),
- the pH measured in a soil suspension:  $pH_{KCl}$  in KCl (1 mol·dm<sup>-3</sup>) solution and  $pH_w$  in distilled H<sub>2</sub>O (at ratio 1:2.5) using potentiometric method,

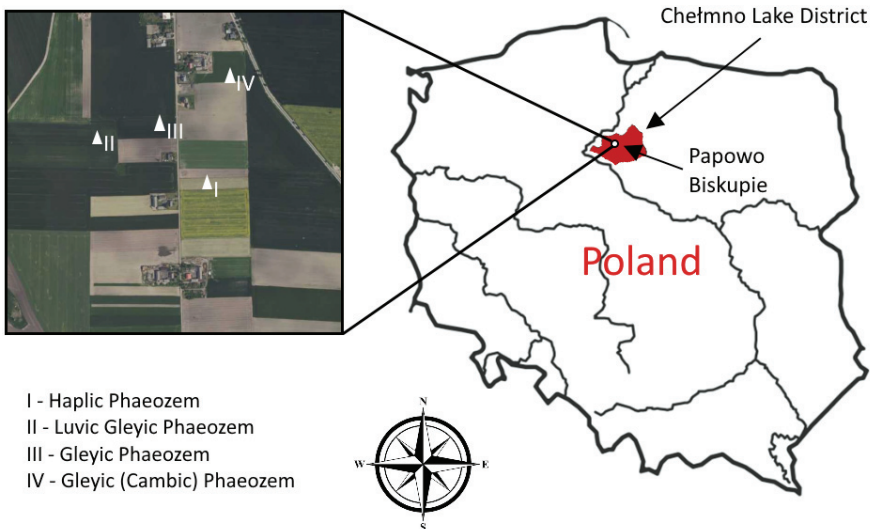


Fig. 1. Study area with soil profiles location

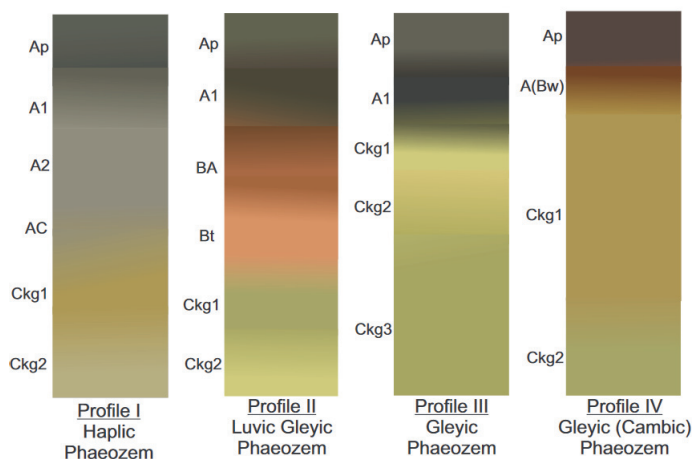


Fig. 2. Schematic morphology of the soils profiles

Table 1.

Elevation, location and relief type of studied profiles

Profile	PSC 2019	WRB 2022	Coordinates	Elevation above sea level (meters)	Relief
I	leached black earths	Haplic Phaeozem	53°24'19.61"N 18°56'63.01"E	86	footslope
II	clay-illuvial black earths	Luvic Gleyic Phaeozem	53°24'31.13"N 18°56'15.00"E	89	flat terrain
III	typical black earths	Gleyic Phaeozem	53°24'32.41"N 18°56'42.47"E	84,5	upper slope
IV	cambic black earths	Gleyic (Cambic) Phaeozem	53°24'45.51"N 18°56'76.05"E	88	shoulder of the slope

Sedimentological indices were used for the lithological characterization of the soil material (the SIEWCA computer program). Sedimentological indices were calculated based on the Folk and Ward classification (Prusinkiewicz and Proszek, 1990):

- mean grain diameter (**GSS**), for particle size fractions from 2.0 mm to <0.002 mm,
- standard deviation (**GSO**) based on the degree of soil material sorting determined,
- skewness (**GSK**), which defines the difference between deviations from the mean,
- kurtosis (**GSP**), as a relative measure of the concentration and flattening of the distribution, determines the distribution and concentration of the value of a variable around the mean.

The soil samples were analysed for the content of free iron oxides ( $Fe_o$ ), which was extracted by means of dithionite-citrate-bicarbonate (DCB) according to Mehra and Jackson's (1960) method, as well as the content of amorphous iron oxides, extracted by means of ammonium oxalate ( $Fe_o$ ) according to Schwertmann's (1964) method. Total content of iron was determined after the mineralization of soils in the mixture of HF and  $HClO_4$  acids (Crock and Severson 1980). Based on the content of  $Fe_a$  and  $Fe_o$ , the content of crystalline iron oxides ( $Fe_c$ ) was calculated using the formula:  $Fe_c = Fe_a - Fe_o$  and the iron oxides activity index was calculated from the  $Fe_o/Fe_a$  ratio. Soil parameters were analyzed

with descriptive statistics (arithmetic mean, minimum, maximum, standard deviation, and coefficient of variation) and the analysis of variance (ANOVA). The significance of differences was evaluated using Tukey's test ( $p < 0.05$ ) for uneven numbers. The calculations were made using Statistica 13.0 (StatSoft Inc, Tulsa, USA).

### 3. Results

The soil material (moist) of the Ap horizons was black, very dark gray and very dark brown in colour (Table 2). The parent material with reductimorphic colours of the gleyic colour pattern (2.5Y, 5Y), were olive brown, pale olive and olive gray and showed features of gleying from groundwater (Table 2). Most horizons contained fine and medium soil aggregates (granular in surface humus horizon and angular and subangular blocky in the underlying part of soil profiles).

Soils were slightly leached with pH from 4.88 to 7.09 in Ap horizons. Soil pH (KCl) was acidic in profile I and slightly acidic in profiles II and IV. Different pH values in soil profiles I, II, and IV were observed in the humus and subsurface horizons, and parent material. The TOC content ranged from 0.81  $g \cdot kg^{-1}$  to 17.72  $g \cdot kg^{-1}$ . In all profiles, its content was highest in the A horizon. The examined soil profiles differed in the thickness of solum horizons, because the parent material in profile III was at

**Table 2.**  
Basic parameters of soils

Profile	Horizon	Depth (cm)	pH		Equivalent $CaCO_3$ (%)	TOC ( $g \cdot kg^{-1}$ )	Matrix colour Munsell charts		Bulk density ( $Mg \cdot m^{-3}$ )
			$H_2O$	1M KCl			dry samples	moist samples	
I	Ap	0–25	5.65	4.88	0.00	12.8	7.5YR 4/2	7.5YR 2.5/1	1.55
	A2	25–45	5.80	5.35	0.00	10.8	10YR 4/1	10YR 2/1	1.85
	A3	45–90	6.63	5.53	0.00	6.3	10YR 5/2	10YR 3/2	1.61
	AC	90–120	6.88	6.02	0.21	5.6	10YR 4/4	10YR 3/4	1.87
	Ckg1	120–135	8.38	7.53	5.29	1.7	10YR 6/4	10YR 4/4	1.91
	Ckg2	135–150	8.31	7.49	4.45	1.1	2.5Y 6/4	2.5Y 4/4	1.93
II	Ap	0–30	6.57	5.94	0.00	14.5	10YR 4/2	10YR 3/1	1.52
	A2	30–59	6.78	5.88	0.00	8.9	10YR 4/2	10YR 2/1	1.63
	BA	59–85	7.06	6.53	0.20	5.3	10YR 4/3	10YR 3/2	1.60
	Bt	85–110	7.52	6.54	0.75	4.6	10YR 5/3	10YR 3/3	1.69
	Ckg1	110–138	8.26	7.48	2.54	1.4	5Y 7/3	5Y 5/3	1.72
	Ckg2	138–150	8.15	7.55	2.35	1.0	5Y 7/2	5Y6/3	1.73
III	Ap	0–25	7.43	7.09	0.64	17.7	10YR 3/1	10YR 2/1	1.58
	A2	25–45	7.75	7.08	0.44	4.5	5Y 3/1	5Y 2.5/1	1.79
	Ckg1	45–70	7.98	7.34	4.03	1.4	5Y 6/3	5Y 5/4	1.74
	Ckg2	70–90	8.26	7.49	8.69	1.3	5Y 7/2	5Y 6/2	1.88
	Ckg3	90–150	8.28	7.49	6.14	1.3	5Y 6/2	5Y 5/2	1.94
IV	Ap	0–25	6.64	5.65	0.00	10.4	10YR 4/2	10YR 2/2	1.76
	AB	25–50	6.64	5.67	0.44	10.0	10YR 4/3	10YR 3/2	1.83
	Ckg1	50–100	8.23	7.37	7.21	2.1	10YR 6/4	10YR 4/4	1.80
	Ckg2	100–150	8.32	7.52	9.09	0.8	2.5Y 7/2	2.5Y 4/4	1.89

TOC – total organic carbon

depth of 45 cm, whereas in profile I it was at a depth of 120 cm. The parent materials of all soils contained CaCO<sub>3</sub> ranging from 2.35% (profile II) to 9.09% (profile IV). However, although a lot of secondary forms of calcium carbonate (profile I, III and IV), Ckg horizons did not meet the protocalcic criteria.

The soil in most genetic horizons was sandy loam in texture (Table 3). Only in the A2 horizon in profile I and in BA and Bt in profile II it was loam. The content of the clay fraction ranged from 9% to 18%. The parent material of the studied soils, which is a glacial deposit rich in CaCO<sub>3</sub>, is genetically homogenous. The homogeneity of the parent material is confirmed by the values of sedimentological indices (very poorly sorted materials). According to Folk and Ward (Prusinkiewicz and Proszek, 1990), GSO values below 0.35 determine very well sorted soil material, values of 0.35–1.00 indicate well sorted material, values of 1.00–2.00 indicate poorly sorted material, and values of 2.00–4.00 are very poorly sorted, while values above 4.00 characterize unsorted soil material. Skewness (GSK) contains information about possible differences between positive and negative deviations from the mean. Skewness has a positive value when the values of a variable are predominantly low (i.e. smaller fractions predominate). The GSK index can be used to determine the dominance of individual fractions in a sample. Prusinkiewicz and Proszek (1990) report that, for a normal (mesokurtic) distribution, the GSP index is 1.00. Values below 1.00 characterize platykurtic distributions, and values above 1.00 are characteristic of leptokurtic

distributions. Unsorted soil material (GSO > 4.0) was found in the surface horizons of profiles I and IV. The skewness (GSK) ranges from 0.25 to 0.65 and indicates the soil material is dominated by smaller-diameter particles.

Unsorted soil material was recorded in the Ap horizons in profile I, the C1kg parent material in profile III, and the Ap and AB horizons in profile IV. The highest degree of sorting (GSO=2.79) was found in the soil sample collected from the C2kg horizon in profile II (Table 4). The mean grain diameter of the studied soils was 0.053 mm in the surface horizons, 0.046 mm in the subsurface horizons, and 0.048 mm in the parent material (Fig. 3).

The content of Fe<sub>t</sub> was lowest in the surface horizons (Ap and A2) of profile III, and highest (25.06 g·kg<sup>-1</sup>) in the Bt horizon of profile II (Table 4). In individual profiles, Fe<sub>a</sub> content was highest in the Bt horizon (5.89 g·kg<sup>-1</sup>) of profile II, the AB horizon (4.88 g·kg<sup>-1</sup>) of profile IV, and the top of the parent material C1kg (4.87 g·kg<sup>-1</sup>). In II and IV soil profiles, iron was removed from the surface horizon to be accumulated in the illuvial horizon.

The soil of the A horizons in profiles I, II and IV was higher in amorphous iron content than was the parent material. Only in profile III was the Fe<sub>o</sub> content found to be highest in the C1kg horizon (1.49 g·kg<sup>-1</sup>). The lowest Fe<sub>c</sub> content was recorded in the surface horizons of the studied soils, i.e. the A2 horizon (0.76 g·kg<sup>-1</sup>) of profile I, the Ap horizon (1.79 g·kg<sup>-1</sup>) of profile II, the Ap horizon of profile III (1.25 g·kg<sup>-1</sup>) and the Ap horizon of profile IV (2.92 g·kg<sup>-1</sup>).

**Table 3.**  
Particle size distribution

Profile	Horizon	Percentage of fractions with diameter (mm)			Texture class (USDA)
		2.0–0.05	0.05–0.02	<0.002	
		I	Ap	59	
	A2	46	40	14	L
	A3	57	29	14	SL
	AC	61	27	12	SL
	Ckg1	62	24	14	SL
	Ckg2	63	24	13	SL
II	Ap	65	26	9	SL
	A2	60	26	14	SL
	BA	46	37	17	L
	Bt	49	33	18	L
	Ckg1	60	27	13	SL
	Ckg2	73	16	11	SL
III	Ap	65	21	14	SL
	A2	72	15	13	SL
	Ckg1	62	22	16	SL
	Ckg2	59	26	15	SL
	Ckg3	62	24	14	SL
IV	Ap	61	24	15	SL
	AB	60	25	15	SL
	Ckg1	59	27	14	SL
	Ckg2	60	28	12	SL

SL – sandy loam, L – loam

**Table 4.**  
Sedimentological parameters (indices) of soil material

Profile	Horizon	Sedimentological indices			
		GSO	GSK	GSP	GSS
I	Ap	4.05	0.33	2.08	0.061
	A2	3.48	0.38	2.01	0.031
	A3	3.49	0.42	1.60	0.038
	AC	3.52	0.30	1.17	0.052
	Ckg1	3.83	0.41	1.42	0.048
	Ckg2	3.70	0.34	1.28	0.054
II	Ap	3.00	0.36	1.32	0.050
	A2	3.89	0.41	1.77	0.047
	BA	3.58	0.34	1.22	0.025
	Bt	3.24	0.65	1.51	0.020
	Ckg1	3.04	0.56	2.19	0.037
	Ckg2	2.79	0.54	2.20	0.053
III	Ap	3.99	0.41	1.76	0.055
	A2	3.56	0.49	2.03	0.059
	Ckg1	4.28	0.40	1.18	0.043
	Ckg2	3.96	0.27	1.01	0.048
	Ckg3	3.62	0.38	1.14	0.045
IV	Ap	4.05	0.38	1.48	0.047
	AB	4.02	0.33	1.25	0.047
	Ckg1	3.56	0.31	0.89	0.043
	Ckg2	3.57	0.25	0.93	0.051

GSO – standard deviation; GSK – skewness; GSP – kurtosis; GSS – mean grain diameter in mm

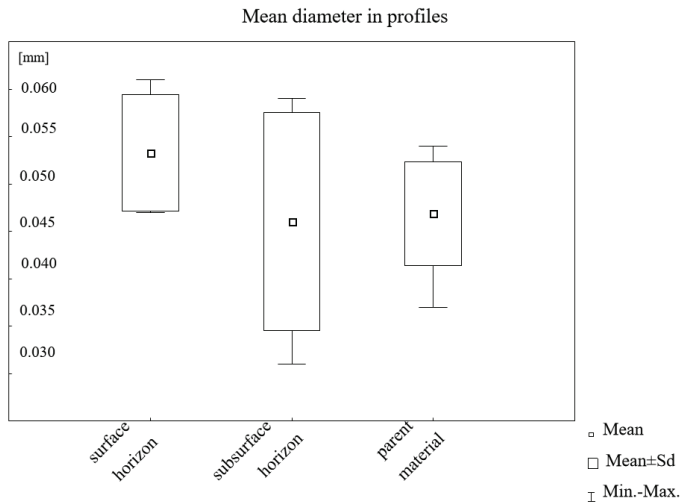


Fig. 3. Mean diameter of soil particles in profiles

The lowest  $Fe_o/Fe_d$  ratio values were found in the parent material of the studied soils, which were rich in crystalline forms of iron (Table 6). The uniformity of content of total iron and its free iron oxides in the parent material of the analysed soils indicates its genetic homogeneity. The highest total iron content  $Fe_t$  was found in Bt and BA horizons. The release of iron in the Ap horizon is typical of chemical weathering, which releases iron from silicate and aluminosilicate structures. Interpreting the content

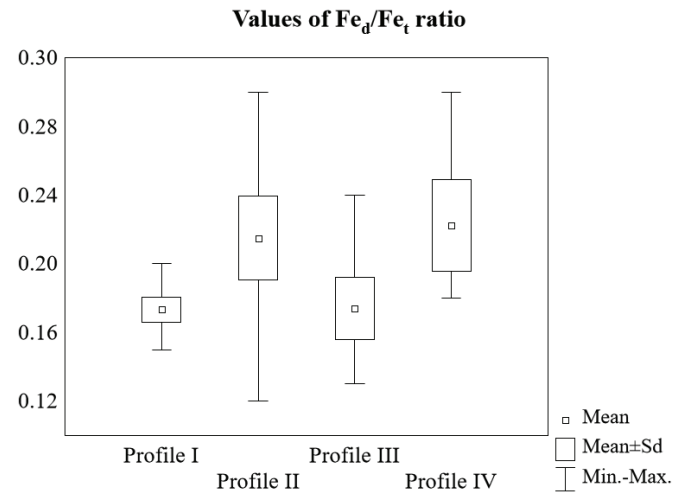


Fig. 4. Mean values of  $Fe_o/Fe_t$  ratio

of individual forms of iron by cluster analysis, the soil material of the arable horizon and the subsurface horizon was found to differ from the parent material (Fig. 4). The soil in the BA and Bt horizons of profile II and AB of profile IV also stood out for being rich in  $Fe_t$  and  $Fe_o$ . The  $Fe_t$  content was lowest in the surface horizons (Ap and A2) of profile III and highest (25.06 g·kg<sup>-1</sup>) in the Bt horizon of profile II (Table 5). Of all profiles,  $Fe_d$  content was highest in the Bt enrichment horizon (5.89 g·kg<sup>-1</sup>) of profile II, the

Table 5.

Forms of iron:  $Fe_t$  – total content of iron;  $Fe_d$  – free iron;  $Fe_o$  – amorphous iron;  $Fe_c$  – crystalline iron ( $Fe_c = Fe_d - Fe_o$ )

Profile	Horizon	$g \cdot kg^{-1}$				$Fe_d/clay$	$Fe_o/Fe_d$	$Fe_d/Fe_t$
		$Fe_t$	$Fe_o$	$Fe_c$	$Fe_d$			
I	Ap	16.11	1.65	1.23	2.88	0.22	0.57	0.18
	A2	17.32	1.90	0.76	2.66	0.19	0.71	0.15
	A3	18.64	1.77	1.24	3.01	0.21	0.59	0.16
	AC	21.03	1.69	2.52	4.21	0.35	0.40	0.20
	Ckg1	21.48	0.52	3.35	3.87	0.28	0.13	0.18
	Ckg2	20.14	0.48	2.94	3.42	0.26	0.14	0.17
II	Ap	12.41	1.14	1.79	2.93	0.33	0.39	0.24
	A2	13.95	1.43	2.77	4.20	0.30	0.34	0.30
	BA	23.69	2.99	2.43	5.42	0.32	0.55	0.19
	Bt	25.06	2.61	3.28	4.89	0.33	0.44	0.23
	Ckg1	20.82	0.83	3.51	4.34	0.33	0.19	0.21
	Ckg2	19.88	0.47	2.00	2.47	0.22	0.19	0.12
III	Ap	11.90	0.76	1.25	2.01	0.14	0.36	0.17
	A2	11.15	0.28	1.54	1.82	0.14	0.15	0.16
	Ckg1	20.42	1.49	3.38	4.87	0.29	0.31	0.24
	Ckg2	20.40	0.26	2.33	2.59	0.17	0.10	0.13
	Ckg3	19.51	0.37	3.01	3.38	0.24	0.11	0.17
IV	Ap	14.33	1.39	2.92	4.31	0.29	0.32	0.30
	AB	23.60	1.38	3.50	4.88	0.32	0.21	0.21
	Ckg1	20.13	0.49	3.62	4.11	0.29	0.11	0.20
	Ckg2	21.98	0.63	3.37	4.00	0.33	0.16	0.18

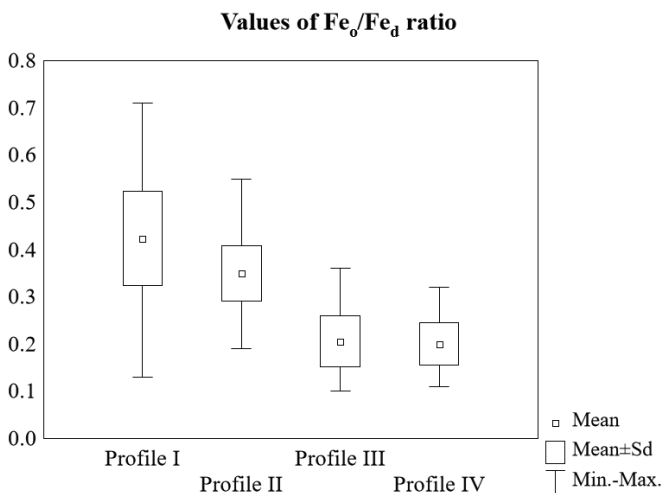


Fig. 5. Mean value of  $Fe_o/Fe_d$  ratio

AB horizon ( $4.88 \text{ g}\cdot\text{kg}^{-1}$ ) of profile IV, the top of the parent material C1kg ( $4.87 \text{ g}\cdot\text{kg}^{-1}$ ) of profile III, and the AC horizon ( $4.21 \text{ g}\cdot\text{kg}^{-1}$ ) of profile I. The soil of surface horizons in profiles I, II and IV was higher in amorphous iron content than was the parent material. Only in profile III was the  $Fe_o$  content found to be highest in the C1kg horizon ( $1.49 \text{ g}\cdot\text{kg}^{-1}$ ). The lowest  $Fe_c$  content was recorded in the surface horizons of the studied soils, i.e. the A2 horizon ( $0.76 \text{ g}\cdot\text{kg}^{-1}$ ) of profile I, the Ap horizon ( $1.79 \text{ g}\cdot\text{kg}^{-1}$ ) of profile II, the Ap horizon ( $1.25 \text{ g}\cdot\text{kg}^{-1}$ ) of profile III and the Ap horizon ( $2.92 \text{ g}\cdot\text{kg}^{-1}$ ) of profile IV. The  $Fe_d/\text{clay}$  ratio values differed little between profiles, ranging from 0.14 in the Ap and A2 horizons of profile III to 0.35 in the AC horizon of profile I. Values of the  $Fe_o/Fe_d$  ratio

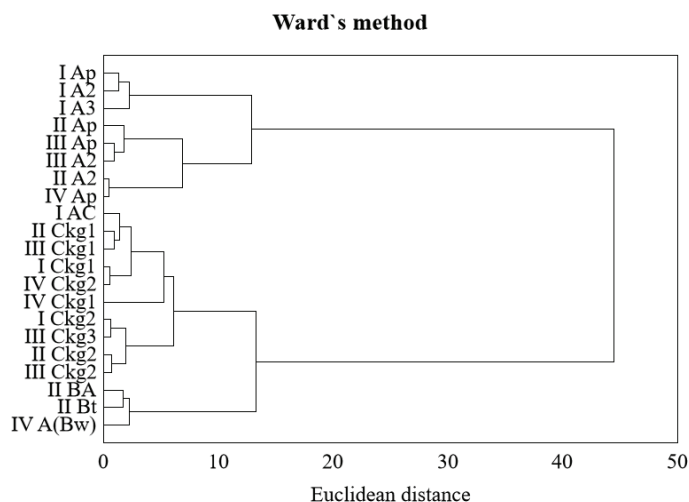


Fig. 6. Cluster analysis for  $Fe_o$ ,  $Fe_d$ ,  $Fe_c$

were lowest in the parent material of the soils, which were rich in crystalline iron forms. The highest shares of amorphous iron relative to  $Fe_d$  were recorded in the soil of the A2 horizon of profile I (0.71). In this profile, the highest mean  $Fe_o/Fe_d$  ratio was recorded (Fig. 5). In profile II, this ratio was highest in the BA and Bt horizons (0.55 and 0.44). The values of the  $Fe_d/Fe_c$  ratio, which describes the degree of weathering of soil material, were similar across all soil profiles (Fig. 6). Interpreting the content of iron forms in the studied profiles, it was found that the soil of genetic horizons containing higher amounts of clay fraction were significantly higher in  $Fe_o$ ,  $Fe_d$  and  $Fe_c$  contents, as confirmed by Pearson correlation coefficient (Fig. 7). This applies to profiles

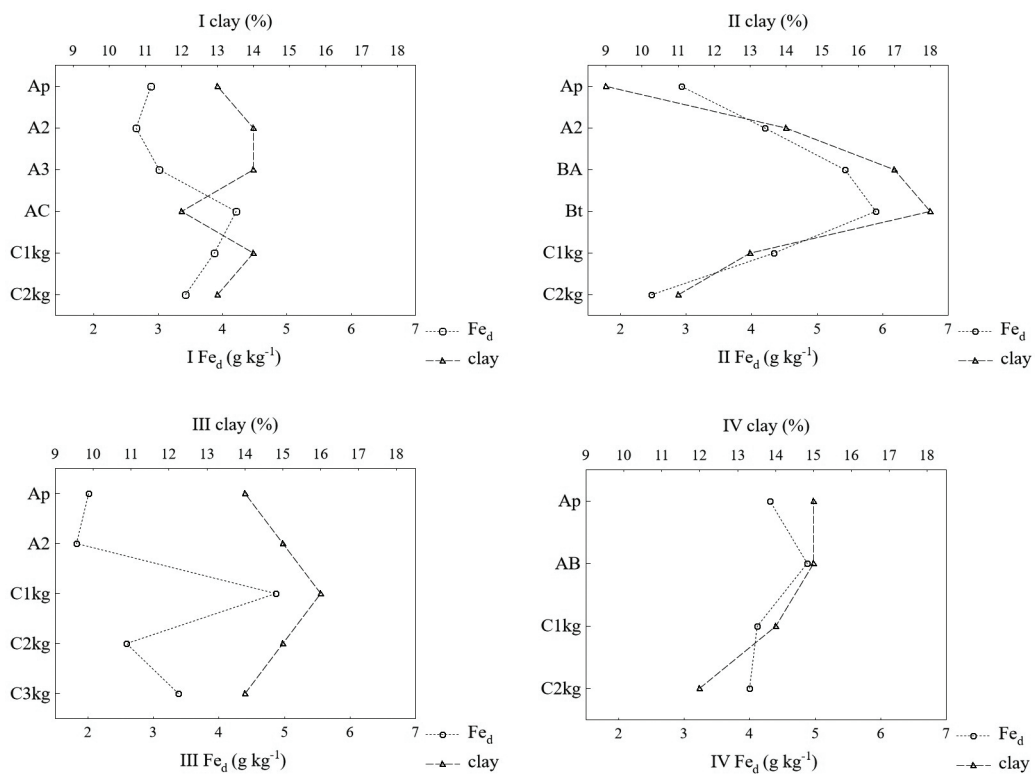


Fig. 7. Distribution of  $Fe_d$  and clay fraction in soil profiles

**Table 6.**Pearson linear correlation coefficient values,  $p < 0.05$ 

Parameter	Fe <sub>a</sub>	Fe <sub>o</sub>	Fe <sub>c</sub>	Clay fraction
Fe <sub>t</sub>	0.68*	0.27	0.59*	0.44*
Fe <sub>a</sub>		0.58*	0.72*	0.59*
Fe <sub>o</sub>				0.49*
Fe <sub>c</sub>				0.30

\* – values of significant correlation coefficient

II, III and IV. A significantly positive correlation was found between total iron content and its Fe<sub>a</sub> and Fe<sub>c</sub> forms. The soil material higher in Fe<sub>a</sub> content contained statistically significantly higher Fe<sub>o</sub> and Fe<sub>c</sub> content (Table 6).

#### 4. Discussion

Soil units are distinguished by type in Polish Classification System and by reference groups in WRB (Systematyka Gleb Polski 2019; IUSS Working Group WRB 2022), based on the classification's definition of the main genetic horizons in the profile and features associated with diagnostic horizons as well as diagnostic features and materials. The accumulation of soil organic matter and reducing conditions caused by groundwaters were key soil-forming processes recorded in the studied soils, as reflected in the classification. Mineralization of organic matter and the leaching of CaCO<sub>3</sub> may occur as a result of drainage and intensive agricultural use. The studied soils were used in a conventional plowing manner, which resulted in the compaction of the subsurface layers. The humus horizon in soil profile I had acidic and slightly acidic pH values. Unfavorable changes in the humus horizon as an effect of soil compaction and a decrease in soil organic matter content and acidification are the most important symptoms of soil degradation (Shah et al., 2017). Hard layers in soils can be formed as a result of the natural soil packing process, and these may occur throughout the topsoil (Singh et al., 2015). An increase in compaction depends mostly on texture (especially the content of clay fraction), bulk density (BD), SOM, and climatic conditions (Gross et al., 2018). The soil organic matter (SOM) content in soil is one of the key arable soil quality criteria (Kögel-Knabner and Amelung, 2021). The amount of SOM as well as its quality parameters and the organic-mineral associations are soil-type and climate-zone specific (Wiesmeier et al., 2019).

The argic horizon in profile II is subordinate in the presence of a deep mollic horizon in the Phaeozems. Profile II shows the features of a secondary soil-forming process with the clay fraction illuviation characteristic of "lessivage". Soils developed from glacial tills characterized by natural poor drainage and waterlogging are found in Poland and are called "black earths". According to the Polish Soil Classification (Kabala et al. 2019a), soils with a mollic horizon and secondary carbonate accumulation below the mollic horizon, and gleyic or stagnic properties, are classified in a black earths type. These soils refer to Phae-

ozems in World Reference Base for Soil Resources (IUSS Working Group WRB 2022).

The analysed profiles had a sandy loam texture. It is a typical soil material from which most of the Phaeozems were formed during the late Vistulian (Weichselian) glaciation (Kobierski and Dąbkowska-Naskręć, 2003b; Kobierski, 2010). The soil cover of the Chełmno Lake District is closely related to the region's lithology and topography. It is an area with a varied landscape, with numerous undulating and flat moraine plateaus built mainly of fine-grained clay and glacial sands (Matecka and Świtoniak, 2020; Świtoniak, 2015; Świtoniak et al., 2016; Wysota, 1993). They cover areas where often-eroded Luvisols occur and in depressions of Phaeozems with redoxymorphic features. Pedon II is distinguished by a marked vertical translocation of the clay fraction within the soil profile. The subsurface Bt horizon in Phaeozem is referred as clay rich zone altered by pedogenesis, mostly due to illuviation of clay fraction and formation of iron oxides. Hristov (2020) noted that clay rich layer formation in Phaeozems is mainly in situ, but also clay illuviation could be cause. This Bt horizon is usually brownish or reddish due to the content of iron oxides, which increases the chroma of the soil material to a degree that it can be distinguished from the other horizons. Phaeozem subtypes with argic and cambic horizon are increasingly being interpreted as indicating that these soils were formed at different times and under conditions that differ from those now prevailing in a given area. This applies to profiles II and IV. Profile II exhibits an accumulation of clay fraction in the Bt horizon and BA transitional horizon, and their soil materials have a distinct brown colour (dry mass 10YR 4/3 and 10YR 5/3). The AB horizon in profile IV is more saturated when wet and redder in hue than the horizon below, indicating that pedogenic features predominate over lithogenic ones. Soil colour is significant with respect to various soil properties, including organic matter contents. The features of the lessivage process can also be seen in the soil material of Profile II, in addition to the basic soil-forming features that define Phaeozems. The morphological features and vertical distribution of clay fractions and free iron oxides in Phaeozems from the Kujawy region in central Poland were noted (Kobierski, Dąbkowska-Naskręć 2003a,b). The mechanism of the lessivage process is based on the leaching of the clay with similar ratios of sand to silt fractions deep down in the soil profiles. Eckmeier et al. (2007) concluded that increasing precipitation and leaching lead to the development of first Haplic, then Cambic and Luvic Chernozems, and finally Luvic Phaeozems. The development of Luvisols is caused by the stronger leaching of clay (Driessen, 2001). Phaeozems are characterized by a humus-rich surface layer, and they are highly arable soils. Soil-forming process of gleyic Phaeozems can develop into Haplic/Luvic Phaeozems or with a Cambic diagnostic horizon. This process was also observed in Phaeozems from the Kujawy region (Kobierski, Dąbkowska-Naskręć 2003). The clay could be translocated into the top of the parent material, which is under the humus horizon. In Profile III, this process was observed.

Transformations of soil material in the AB horizon of profile IV differ from one another in nature and include the processes of aluminosilicates weathering, which can be affected by roots and microorganisms. This subsurface horizon lacks features of clay



fraction illuviation and exhibits the properties of Bw horizon. The Bw horizon can have a range of pedogenic features resulting from *in-situ* processes: brown colour and finer texture in the middle part of a soil profile in comparison to the parent material → weathering → enrichment of Fe-oxides → horizon Bw. In soils with a cambic diagnostic horizon, the soil-forming process affects the Fe content through non-illuvial accumulation of all iron forms. It is difficult to clearly determine what proportion of the iron in the Bt horizon of profile II and AB horizon of profile IV was due to illuvial accumulation of this metal. Nevertheless, the content of iron oxides in the AB horizon of profile IV was slightly lower than in the Bt of profile II. The process of leaching clay fraction leads to enrichment of illuvial in free iron oxides. The comigration of clay fraction and iron oxides was confirmed by a significant correlation of  $Fe_d$  and clay (Fig. 3, 4, 5). Haidouti and Massas (1998) found a similar relationship between those parameters. The profile distribution of Fet was similar to the distribution of the clay fraction, which can indicate a secondary illuviation of iron to the Bt horizon together with the clay fraction in profile II. Iron oxides, although accounting for an inconsiderable percentage of soil materials, have considerable influence on soil properties. The relatively high content of  $Fe_t$  identified in the gleyic parent material originated from the presence of clay minerals containing iron in its crystalline structures (Kobierski and Dąbkowska-Naskręt, 2003b). The intensity of the weathering process and the course of the soil-forming process can be assessed based on the content of iron forms in the soil profile. Low values of the  $Fe_d/Fe_t$  ratio indicate that all those tested are young soils. The degree of weathering of soils formed in similar soil and climatic conditions correlates with their age (Ardiuno et al., 1986). The process of leaching clay leads to the depletion of the eluvial horizon and the enrichment of illuvial in free iron oxides. The morphological characteristics reflect the existence of the Black earths subtype. A cambic or argic horizon with a characteristic accumulation of clay fraction and iron can form under a mollic horizon. These soils are usually located in higher-elevation areas. Associations of black earths with Luvisols are also very often found. The dynamics of iron transformations can be determined based on the content of dithionite- ( $Fe_d$ ) and oxalate-extractable ( $Fe_o$ ) iron, as well as the  $Fe_o/Fe_d$  ratio (McFadden and Hendricks, 1985). Conclusions as to the transformations of iron in the soil can be drawn based on the  $Fe_o/Fe_d$  ratio, as it determines the relationship between the content of the most active forms of iron and its non-silicate forms (Schwertmann, 1988). The value of this index in the parent material ranged from 0.10 to 0.71. The values of the  $Fe_o/Fe_d$  index, which describes the degree of activity of iron oxides, were highest in the surface and subsurface horizons of the profiles. This indicates that the conditions in the surface layer of these soils were unfavourable to the crystallization of oxides.  $Fe_d$  may occur in soil in  $Fe_c$  or  $Fe_o$ , which are the most labile and active forms of iron. Increasing  $Fe_o/Fe_d$  ratios indicate the formation of organic complexes, hindering the crystallization of iron oxides. Increased  $Fe_o$  contents could be caused by the presence of organic matter and temporary anaerobic conditions, which inhibit the crystallization of iron oxides. Lower values of the  $Fe_o/Fe_d$  ratio in the parent material of the soils derived from glaciolimnic materials than in their

solum suggest more iron oxide crystallization (Orzechowski et al. 2018). In the analyzed soils, the lowest  $Fe_o$  content was determined in the parent material containing  $CaCO_3$ . This indicates that the specific geochemical conditions of the analyzed Pheozems may affect the formation of iron oxides. Low contents of  $Fe_d$  and  $Fe_o$  may be an indirect indicator of the presence of reduction (anaerobic) conditions. Iron in reduced form ( $Fe^{2+}$ ) is more mobile than iron in oxidized state ( $Fe^{3+}$ ) (Cornell and Schwertmann, 1996). Therefore, the soil material with low contents of  $Fe_d$  and  $Fe_o$  may have been depleted in iron by the reduction of iron to  $Fe^{2+}$ . Anaerobic conditions might cause the reduction of structural Fe, which in turn affects the changes in chemical and physical properties of clay minerals (Stucki, 2011). An essential parameter indicating the soil-forming process is the degree of iron mobilisation. Low contents of amorphous forms of iron are reflected in the analysed soils by low index of crystallinity. Similarly low values of this index were determined by Mocek (1988).

## 5. Conclusions

All the profiles were characterized by similar degrees of weathering of the soil material, which was determined on the basis of the  $Fe_d/Fe_t$  ratio. The soils also demonstrate a low value of iron mobilization, as confirmed by the values of the  $Fe_d/Fe_t$  ratio.

The higher  $Fe_o/Fe_d$  ratios in the soil material of surface and subsurface horizons indicate a greater activity of iron in soil-forming processes. The  $Fe_d/clay$  ratio indicates comigration of clay fraction and free iron oxides. It can be concluded that this is due to over-draining of the studied soils. Based on the statistical analysis, a significantly positive correlation between the content of clay fraction and all the iron forms determined was found. The soil parent material contained more  $Fe_c$  than the surface horizons, which suggests that the process of iron oxide crystallisation was not favoured in the humic horizon.

The distribution of iron forms in soil profiles mostly depends on pedogenesis, hence identifying iron forms and interpreting analysis results aid in the proper classification of soils.

## References

- Aitkenhead, M.J., Coull, M., Towers, W., Hudson, G., Black, H.I.J., 2013. Prediction of soil characteristics and color using data from the National Soils Inventory of Scotland. *Geoderma* 200-201, 99-107. <https://doi.org/10.1016/j.geoderma.2013.02.013>
- Arduino, E., Berberis, E., Marsan, F.A., Zanini, E., Franchini, M., 1986. Iron oxides and clay minerals within profiles as indicators of soil age in Northern Italy. *Geoderma* 37, 45-55.
- Bednarek, R., Pokojska, U., 1996. Diagnostyczne znaczenie niektórych wskaźników chemicznych w badaniach paleopedologicznych. *Mat. Konf. Metody badań paleopedologicznych i wykorzystanie gleb kopalnych w paleopedologii*, 25-29.
- Bigham, J.M., Heckendorn, S.E., Jaynes, W.F., Smeck, N.E., 1991. Stability of iron oxides in two soils with contrasting colors. *Soil Science Society of America Journal* 55, 1485-1492. <https://doi.org/10.2136/sssaj1991.03615995005500050048x>

- Bockheim, J.G., Gennadiyev, A.N., Hammer, R.D., Tandarich, J.P., 2005. Historical development of key concepts in pedology. *Geoderma* 124(1–2), 23–36. <https://doi.org/10.1016/j.geoderma.2004.03.004>
- Chojnicki, J., Brzozowska, A., Hryciuk, A., Marczak, R., 2010. Formy żelaza, glinu i manganu jako wskaźniki niektórych procesów glebotwórczych w glebach rezerwatu „Rybitew” Kampinoskiego Parku Narodowego, *Roczniki Gleboznawcze – Soil Science Annual* 61(2), 29–36.
- Cornell, R.M., Schwertman, U., 2003. The iron oxides: Structure, properties, reactions, occurrence and uses. 2nd edn. VCH, Weinheim, Germany.
- Dąbkowska-Naskręt, H., Kobierski, M., Długosz, J., 1998. Characteristics of clay minerals in black earths from Kujawy region. *Roczniki Gleboznawcze – Soil Science Annual* 49(1/2), 45–52.
- Degórski, M., 2011. The relationships between different forms of iron and aluminium in soils as indicators of soil-cover development on India's Cherrapunji Spur (Meghalaya Plateau). *Geographia Polonica* 84(1), 61–73. <https://doi.org/GPol.2011.1.5>
- Długosz, J., Orzechowski, M., Kobierski, M., Smólczyński, S., Zamorski, R., 2009. Clay minerals from Weichselian glaciolimnic sediments of the Sępopolska Plain (NE Poland). *Geologica Carpathica* 50(3), 263–267. <https://doi.org/10.2478/v10096-009-0018-z>
- Drewnik, M., Skiba, M., Szymański, W., Żyła, M., 2014. Mineral composition vs. soil forming processes in loess soils – a case study from Kraków (southern Poland). *Catena* 119, 166–173. <https://doi.org/10.1016/j.catena.2014.02.012>
- Driessen, P., Deckers, J., Spaargaren, O., Nachtergaele, F.O., 2001. Lecture Notes on the Major Soils of the World. World Soil Resources Report, vol. 94. FAO, Wageningen.
- Eckmeier, E., Gerlach, R., Gehrt, E., Schmidt, M.W.I., 2007. Pedogenesis of Chernozems in central Europe – A review. *Geoderma* 139, 288–299. <https://doi.org/10.1016/j.geoderma.2007.01.009>
- Gliński, J., Stępniewska, Z., 1986. Wskaźnik odporności gleb na redukcję. *Zeszyty Problemowe Postępów Nauk Rolniczych* 315, 81–94.
- Gross, C.D., Harrison, R.B., 2018. Quantifying and comparing soil carbon stocks: Underestimation with the core sampling method. *Soil Science Society of America Journal* 82(4), 949–959. <https://doi.org/10.2136/sssaj2018.01.0015>
- Habel, A.Y., Kaczmarek, Z., Mocek, A., 2007. Selected physical and chemical properties and the structure condition of phaeozems formed from different parent materials. Part I. Physical and chemical properties. *Journal of Research and Applications in Agricultural Engineering* 52(3), 45–49.
- Haidouti, C., Massas, I., 1998. Distribution of iron and manganese oxides in Haploxeralfs and Rhodoxeralfs and their relation to the degree of soil development and soil colour. *Zeitschrift für Pflanzenernährung und Bodenkunde* 161(2), 141–145.
- Hristov, B., 2020. Some physicochemical properties of phaeozems in Bulgaria. *Forestry Ideas* 26, 2(60), 520–527.
- Hu, P., Liu, Q., Torrent, J., Barrón, V., Jin, C., 2013. Characterizing and quantifying iron oxides in Chinese loess/paleosols: Implications for pedogenesis. *Earth and Planetary Science Letters* 369–370, 271–283. <https://doi.org/10.1016/j.epsl.2013.03.033>
- IUSS Working Group WRB, 2022. World Reference Base for Soil Resources. International soil classification system for naming soils and creating legends for soil maps. 4th edition. International Union of Soil Sciences (IUSS), Vienna, Austria.
- Jankowski, M., Kruczkowska, B., Bednarek, R., 2011. Topographical inversion of sandy soils due to local conditions in Northern Poland. *Geomorphology* 135 (3–4), 277–283. [10.1016/j.geomorph.2011.02.005](https://doi.org/10.1016/j.geomorph.2011.02.005)
- Jankowski, M., 2014a. The evidence of lateral podzolization in sandy soils of Northern Poland. *Catena* 112, 139–147. <https://doi.org/10.1016/j.catena.2013.03.013>
- Jankowski, M., 2014b. Bielicowanie jako wtórny proces w glebach rdzawych Brodnickiego Parku Krajobrazowego, [in:] M. Świtoniak, M. Jankowski, R. Bednarek (red.), *Antropogeniczne przekształcenia pokrywy glebowej Brodnickiego Parku Krajobrazowego*, Wydawnictwo Naukowe UMK, Toruń, 9–24.
- Jaworska, H., Dąbkowska-Naskręt H., Kobierski, M., 2014. The influence of litho- and pedogenic process on Luvisols formation of selected area of Vistula Glaciation. *Geological Quarterly* 58(4), 685–694. <https://doi.org/10.7306/gq.1175>
- Jaworska, H., Dąbkowska-Naskręt H., Kobierski, M., 2016. Iron oxides as weathering indicator and the Origin Of Luvisols From The Vistula Glaciation Region. *Journal of Soils and Sediments* 16, 396–404. <https://doi.org/10.1007/s11368-015-1201-8>
- Jelić, M.Ž., Milivojević, J.Ž., Trifunović, S.R., Đalović, I.G., Milošev, D.S., Šeremešić, S.I., 2011. Distribution and forms of iron in the Vertisols of Serbia. *Journal of Serbian Chemical Society* 76(5), 781–794. <https://doi.org/10.2298/JSC100619068J>
- Kabała, C., 2019. Chernozem (czarnoziem) – Soil of the year 2019 in Poland. Origin, classification and properties of Chernozems in Poland. *Soil Science Annual* 70(3), 184–192. <https://doi.org/10.2478/ssa-2019-0016>
- Kabała, C., Charzyński, P., Chodorowski, J., Drewnik, M., Glina, B., Greinert, A., Hulisz, P., Jankowski M., Jonczak, J., Łabaz, B., Łachacz, A., Marzec, M., Mendiak, Ł., Musiał, P., Musielok, Ł., Smreczak, B., Sowiński, P., Świtoniak, M., Uzarowicz, Ł., Waroszewski, J., 2019a. Polish Soil Classification, 6th edition - principles, classification scheme and correlations. *Soil Science Annual* 70(2), 71–97.
- Kabała, C., Charzyński, P., Chodorowski, J., Drewnik, M., Glina, B., Greinert, A., ... & Waroszewski, J., 2019. Systematyka gleb Polski. Wrocław: Wydawnictwo Uniwersytetu Przyrodniczego we Wrocławiu.
- Kabała, C., Charzyński, P., Czigány, Sz., Novák, T.J., Saksa, M., Świtoniak, M., 2019b. Suitability of World Reference Base for Soil Resources (WRB) to describe and classify chernozemic soils in Central Europe. *Soil Science Annual* 70 (3), 244–257. <https://doi.org/10.2478/ssa-2019-0022>
- Kabala, C., Muszytyfaga, E., Jary, Z., Waroszewski, B., Kobierski, M., 2022. Glossic planosols in the postglacial landscape of central Europe: Modern polygenetic soils or subaerial palaeosols? *Geoderma* 426 (15), 116101. <https://doi.org/10.1016/j.geoderma.2022.116101>
- Kaczmarek, Z., Gajewski, P., Mocek, A., Owczarzak, O., Glina, B., 2015. Physical and water properties of selected Polish heavy soils of various origins. *Soil Science Annual*, 66(4), 191–197. <https://doi.org/10.1515/ssa-2015-0036>
- Kobierski, M., 2010. Profile distribution of iron in arable soils formed on glacial till from Inowrocławska Plain, Poland. W: *Physical, chemical and biological processes in soils*. Szajdak, L., W., Karabanow, A., K., [red] Institute for Agricultural and Forest Environment, Polish Academy of Science. Poznań, 305–322. <https://doi.org/10.5601/jelem.2017.22.4.1413>
- Kobierski, M., Dąbkowska-Naskręt, H., 2003. Skład mineralogiczny i wybrane właściwości fizykochemiczne zróżnicowanych typologicznie gleb Równiny Inowrocławskiej. Cz. II. Skład mineralogiczny frakcji ilastej. *Roczniki Gleboznawcze – Soil Science Annual* 54 (4), 29–44.
- Kobierski, M., Długosz, J., 2011. Wpływ pedogenezy na skład mineralogiczny frakcji ilastej gleb wytworzonych z gliny zwałowej. *Roczniki Gleboznawcze – Soil Science Annual* 62(1), 91–103.
- Kobierski, M., Kondratowicz-Maciejewska, K., Kociniewska, K., 2015. Soil quality assessment of Phaeozems and Luvisols from the Kujawy region (central Poland). *Roczniki Gleboznawcze – Soil Science Annual* 66(3), 111–118. <https://doi.org/10.1515/ssa-2015-0026>
- Kögel-Knabner, I., Amelung, W., 2021. Soil organic matter in major pedogenic soil groups. *Geoderma* 384, 114785. <https://doi.org/10.1016/j.geoderma.2020.114785>
- Konecka-Betley, K., Czepinska-Kamińska, D., Janowska, E., Okołowicz, M., 2002. Gleby stref: ochrony ścisłej i częściowej w Rezerwacie Biosfery Puszcza Kampinowska. *Roczniki Gleboznawcze – Soil Science Annual* 53(3–4), 5–21.

- Łabaz, B., Kabała, C., 2014. Origin, properties and classification of black earths in Poland. *Soil Science Annual* 65(2), 80–90. <https://doi.org/10.2478/ssa-2014-0012>
- Łabaz, B., Kabała, C., Dudek, M., Waroszewski, J., 2019. Morphological diversity of chernozemic soils in south-western Poland. *Soil Science Annual* 70(3), 211–224. <https://doi.org/10.2478/ssa-2019-0019>
- Łabaz, B., Muszyfaga, E., Waroszewski, J., Bogacz, A., Jezierski, P., Kabała, C., 2018. Landscape-related transformation and differentiation of Chernozems – Catenary approach in the Silesian Lowland, SW Poland. *Catena*, 161, 63–76. <https://doi.org/10.1016/j.catena.2017.10.003>
- Matecka, P., Świtoniak, M., 2020. Delineation, characteristic and classification of soils containing carbonates in plow horizons within young moraine areas. *Soil Science Annual* 71(1), 23–36. <https://doi.org/10.37501/soilsa/121489>
- McFadden, L.D., Hendricks, D.M., 1985. Changes in the content and composition of pedogenic iron oxyhydroxides in a chronosequence of soils in southern California. *Quaternary Research* 23, 189–204.
- Mocek, A., 1988. Żelazo w vertisolach i mollisolach okolic Shahrzoor i Raniya w północno-wschodniej części Iraku. *Roczniki Gleboznawcze – Soil Science Annual* 39(3), 45–55.
- Orzechowski, M., Smólczyński, S., Długosz, J., Kalisz, B., Kobierski, M., 2018. Content and distribution of iron forms in soils formed from glaciolimnic sediments, in ne Poland. *Journal of Elementology* 23, 729–744. <https://doi.org/10.5601/jelem.2017.22.4.1413>
- Prusinkiewicz, Z., Proszek, P., 1990. Program komputerowej interpretacji wyników analizy uziarnienia gleb – TEKSTURA. *Roczniki Gleboznawcze – Soil Science Annual* 41(3/4), 5–16.
- Roden, E., Sobolev, D., Glazer, B., Luther, G., 2004. Potential for microscale bacterial Fe redox cycling at the aerobic-anaerobic interface. *Geomicrobiology Journal* 21, 379–391. <https://doi.org/10.1080/01490450490485872>
- Różański, S., Bartkowiak, A., Jaworska, H., 2013. Forms of iron as an indicator of pedogenesis in profiles of selected soil types of the northern area of kujawsko-pomorskie province, Poland. *Soil Science Annual* 64(3), 98–105. <https://doi.org/10.2478/ssa-2013-0018>
- Scheinost, A.C., Schwertmann, U., 1999. Color identification of iron oxides and hydroxysulfates: use and limitations. *Soil Science Society of America Journal* 63(5), 1463–1471.
- Schwertmann, U., 1964. Differenzierung der Eisenoxide des Bodens durch Extraktion mit Ammoniumoxalat-Lösung. *Z. Pfl. Ernähr. Dung. Bodenk.* 105, 194–202.
- Schwertmann, U., 1988. Occurrence and formation of iron oxides in various pedoenvironments. In: *Iron in Soils and Clay Minerals*, 261–301.
- Schwertmann, U., Teylor, R.M., 1989. Iron oxides. In: Dixon J.B. et al. (eds.). *Minerals in Soil Environments*. ASA, Madison, 379–438.
- Shah, A.N., Tanveer, M., Shahzad, B., Yang, G., Fahad S., Ali, S., Bukhari, M.A., Tung, S.A., Hafeez A., Souliyanonh B., 2017. Soil compaction effects on soil health and crop productivity: an overview. *Environmental Science and Pollution Research* 24, 10056–10067. <https://doi.org/10.1007/s11356-017-8421-y>
- Singh, J., Salaria, A., Kaul, A., 2015. Impact of soil compaction on soil physical properties and root growth: A review. *International Journal of Food, Agriculture & Veterinary Sciences* 5, 1, 23–32.
- Stucki, J.W., Goodman, B.A., Schwertmann, U., (Eds.), 1988. *Iron in Soils and Clay Minerals*. D. Reidel, Dordrecht, 893.
- Świtoniak, M., 2015. Issues relating to classification of colluvial soils in young morainic areas (Chełmno and Brodnica Lake District, northern Poland). *Soil Science Annual* 66(2), 57–66. <https://doi.org/10.1515/ssa-2015-0020>
- Świtoniak, M., Kabała, C., Karklins, A., Charzyński, P., Hulisz, P., Mendyk, Ł., Michalski, A., Novák, T.J., Penížek, V., Reintam, E., Repe, B., Saksa, M., Vaisvalavičius, R., Waroszewski, J., 2018. Guidelines for Soil Description and Classification Central and Eastern European Students' Version. Polish Society of Soil Science, Toruń, 1–286.
- Świtoniak, M., Mroczek, P., Bednarek, R., 2016. Luvisols or Cambisols? Micromorphological study of soil truncation in young morainic landscapes – Case study: Brodnica and Chełmno Lake Districts (North Poland). *Catena* 136, 583–595. <https://doi.org/10.1016/j.catena.2014.09.005>
- Targulian, V.O., Krasilnikov, P.V., 2007. Soil system and pedogenic processes: Self-organization, time scales, and environmental significance. *Catena* 71(3), 373–381. <https://doi.org/10.1016/j.catena.2007.03.007>
- Thompson, A., Chadwick, O.A., Rancourt, D.G., Chorover, J., 2006. Iron-oxide crystallinity increases during soil redox oscillations. *Geochimica and Cosmochimica Acta* 70(7), 1710–1727. <https://doi.org/10.1016/j.gca.2005.12.005>
- Vodyanitskii, Y.N., Kirillova, N.P., Manakhov, D.V., Karpukhin, M.M., 2018. Iron compounds and the color of soils in the Sakhalin island. *Eurasian Soil Science* 51(2), 163–175. <https://doi.org/10.1134/S1064229318020138>
- Wiesmeier, M., Urbanski, L., Hobley, E.U., Lang, B., Lützow, M., Marin-Spiotta, E., Wesemael, B., Rabot, E., Ließ, M., Garcia-Franco, N., Wollschläger, U., Vogel, H.-J., Kögel-Knabner, I., 2019. Soil organic carbon storage as a key function of soils – A review of drivers and indicators at various scales. *Geoderma* 333, 149–162. [doi:10.1016/j.geoderma.2018.07.026](https://doi.org/10.1016/j.geoderma.2018.07.026)
- Wysota, W., 1993. Model kształtowania rzeźby subglacjalnej w środkowo-wschodniej części Pojezierza Chełmińsko-Dobrzyńskiego. *Mat. II Seminarium: Geneza, litologia i stratygrafia utworów czwartorzędowych*, Poznań.
- Zagórski, Z., 1996. Granulometryczne wskaźniki procesów pedo- i litogenyzy w glebach niejednorodnych wytworzonych z osadów glacialnych. *Roczniki Gleboznawcze – Soil Science Annual* 47, 125–135.
- Zhang, X., W., Kong, L., W., Cui, X., L., Yin, S., 2016. Occurrence characteristics of free iron oxides in soil microstructure: evidence from XRD, SEM and EDS. *Bulletin of Engineering Geology and the Environment* 75, 1493–1503. <https://doi.org/10.1007/s10064-015-0781-2>

## Rozmieszczenie form żelaza w różnych typach czarnych ziem Pojezierza Chełmińskiego jako wskaźnik procesu glebotwórczego

### Słowa kluczowe

Czarne ziemie  
Żelazo  
Procesy glebotwórcze  
Phaeozems  
Proces glejowy

### Streszczenie

Ważną częścią badań gleboznawczych jest klasyfikacja gleb. Wielu gleboznawców zwróciło szczególną uwagę na różne zależności związane z zawartością i rozmieszczeniem form żelaza w profilu glebowym. Pozwala to na określenie jednostki taksonomicznej zgodnie z klasyfikacją gleb. Celem badań była ocena rozmieszczenia form żelaza jako wskaźnika procesów glebotwórczych w czterech profilach czarnych ziem użytkowanych rolniczo. Przedmiotem badań były gleby wytworzone z osadów lodowcowych na Pojezierzu Chełmińskim (północna Polska). Na podstawie opisu morfologicznego określono je jako Phaeozems: Haplic Phaeozems, Luvic Gleyic Phaeozems, Gleyic Phaeozems i Gleyic (Cambic) Phaeozems. Poziome glebowe zostały opisane zgodnie z wytycznymi FAO. Próbkę gleby analizowano pod kątem zawartości wolnych tlenków żelaza ( $Fe_d$ ) zgodnie z metodą Mehry i Jacksona, a także zawartości amorficznych tlenków żelaza ( $Fe_o$ ) zgodnie z metodą Schwertmanna. Całkowitą zawartość żelaza oznaczono po mineralizacji gleb w mieszaninie kwasów HF i  $HClO_4$ . Na podstawie zawartości  $Fe_d$  i  $Fe_o$  obliczono zawartość krystalicznych tlenków żelaza ( $Fe_c$ ) przy użyciu wzoru:  $Fe_c = Fe_d - Fe_o$ , a wskaźnik aktywności tlenków żelaza obliczono na podstawie stosunku  $Fe_o/Fe_d$ . Zawartość  $Fe_c$  była najwyższa w poziomie Bt profilu II. W poszczególnych profilach zawartość  $Fe_d$  była najwyższa w poziomie Bt Gleyic Phaeozem i poziomie AB Gleyic (Cambic) Phaeozem. W Luvic Gleyic Phaeozem i Gleyic (Cambic) Phaeozem żelazo było usuwane z poziomu powierzchniowego i gromadzone w poziomie iluwialnym. Jednorodność zawartości żelaza całkowitego i jego wolnych tlenków w materiale macierzystym analizowanych gleb wskazuje na ich jednorodność genetyczną. Uwalnianie żelaza w poziomie Ap jest charakterystyczne dla wietrzenia chemicznego. Zależność pomiędzy zawartością  $Fe_o$  i  $Fe_d$  określa stopień krystalizacji wolnych tlenków żelaza. Na podstawie analizy statystycznej stwierdzono istotnie dodatnią korelację pomiędzy zawartością frakcji ilastej a wszystkimi oznaczonymi formami żelaza. Wszystkie profile charakteryzowały się podobnym stopniem zwietrzenia materiału glebowego, który określono na podstawie stosunku  $Fe_d/Fe_c$ . Gleby wykazują również niską wartość mobilizacji żelaza, co potwierdzają wartości stosunku  $Fe_d/Fe_c$ . Oznaczanie form żelaza i interpretacja wyników analiz pomagają w prawidłowej klasyfikacji gleb, ponieważ rozmieszczenie form żelaza w profilach glebowych zależy głównie od pedogenezy.